

Article

On the Importance of H-Bonding Interactions in the Enclathration of Boric Acids in Na(I) Polymers: Experimental and Theoretical Studies

Trishnajyoti Baishya¹, Kamal K. Dutta¹, Antonio Frontera^{2,*}, Rosa M. Gomila², Miquel Barceló-Oliver²
and Manjit K. Bhattacharyya^{1,*}

¹ Department of Chemistry, Cotton University, Guwahati 781001, Assam, India; baishyatrishnajyoti@gmail.com (T.B.); chm2291001_kamal@cottonuniversity.ac.in (K.K.D.)

² Departament de Química, Universitat de les Illes Balears, Crta de Valldemossa km 7.7, 07122 Palma de Mallorca, Spain; rosa.gomila@uib.es (R.M.G.); miquel.barcelo@uib.es (M.B.-O.)

* Correspondence: toni.frontera@uib.es (A.F.); manjit.bhattacharyya@cottonuniversity.ac.in (M.K.B.)

Abstract: Two Na(I) coordination polymers, namely, $\{\text{Na}(\text{BA})_2(\mu\text{-H}_2\text{O})_2\}_n\{\text{adp}\}_n$ (**1**) and $\{[\text{Na}_2(\mu\text{-BA})(\mu\text{-fum})(\mu\text{-H}_2\text{O})_4](\text{BA})\}_n$ (**2**) (where, BA = boric acid, adp = adipic acid, fum = fumarate), were prepared and characterized using elemental analysis, TGA, FT-IR, and single-crystal X-ray diffraction techniques. Various unconventional supramolecular interactions, i.e., $\text{CH}\cdots\text{HC}$ and parallel $\text{CO}\cdots\text{CO}$ interactions, stabilize the layered assembly of compound **1**. Interesting dual enclathration of BA molecules within the supramolecular host cavities formed by $\text{O-H}\cdots\text{O}$ and $\text{C-H}\cdots\text{C}$ interactions stabilizes the crystal structure of compound **2**. The H-bonding interactions in **1** and **2** were further studied theoretically using the quantum theory of atoms in molecules (QTAIM) and the noncovalent interaction plot (NCI Plot) computational tools. The energy of the H-bonds was estimated using the potential energy density at the bond critical points. Theoretical calculations confirmed the presence of $\text{O-H}\cdots\text{O}$ H-bonding interactions in both compounds, forming structure-guiding $R_2^2(8)$ synthons relevant for the stability of the compounds.

Keywords: Na(I) polymers; parallel $\text{CO}\cdots\text{CO}$; dual enclathration; H-bonding; QTAIM; NCI



Citation: Baishya, T.; Dutta, K.K.; Frontera, A.; Gomila, R.M.; Barceló-Oliver, M.; Bhattacharyya, M.K. On the Importance of H-Bonding Interactions in the Enclathration of Boric Acids in Na(I) Polymers: Experimental and Theoretical Studies. *Crystals* **2023**, *13*, 895. <https://doi.org/10.3390/cryst13060895>

Academic Editor: Ana M. Garcia-Deibe

Received: 30 April 2023

Revised: 20 May 2023

Accepted: 25 May 2023

Published: 30 May 2023



Copyright: © 2023 by the authors. Licensee MDPI, Basel, Switzerland. This article is an open access article distributed under the terms and conditions of the Creative Commons Attribution (CC BY) license (<https://creativecommons.org/licenses/by/4.0/>).

1. Introduction

Coordination polymers represent the supramolecular architecture of metal ions and organic moieties that extends in association with covalent bonding, as well as supramolecular contacts [1–3]. In the current research era, the design and synthesis of coordination polymers involving supramolecular interactions has attracted immense attention owing to their interesting physical, chemical properties, and potential applications [4,5]. Although coordination polymers involving transition metals bridged by organic ligands have been well explored [6,7], examples of polymers with s-block elements such as sodium are still scarce in the literature. The strategic synthesis of coordination polymers of such elements is still challenging, which may be due to various factors such as varying coordination number, size of the binding partners, and electrostatic interactions between the ligands and the metal ions [8].

The design of boron-based compounds has received a great deal of interest because of their potential utilities as boron-containing drugs and materials for medical diagnostics [9,10]. Boron compounds can be used as modulators for the bioactivity of biomolecules, in boron capture neutron therapy (BNCT) for drug delivery, and in molecular modeling of drug design [11,12]. Boric acid has been effectively utilized as a building block to construct a variety of compounds with interesting structural topologies [13,14]. Cebula et al. recently highlighted the importance of supramolecular assemblies of boron-mediated anionic clusters and their applications in biological fields [15]. In an organic crystal of 4-

pyridinylboronic acid, B \cdots Cl σ -hole triel bonding interactions were observed, established using various computational tools [16].

To understand the role of noncovalent contacts in self-assembly processes, innumerable efforts have been undertaken due to their potential applications in a wide range of fields such as catalysis, crystal engineering, pharmaceutical design, molecular biology, and molecular recognition [17–19]. Although supramolecular interactions are weaker than covalent bonds, their large numbers and cumulative effects make them potential candidates in the design of crystal structures [20,21]. H-bonding interactions can be considered as the most common which play crucial roles in molecular self-assembly processes [22], as well as in the stabilization of biomolecules such as -DNA and proteins (Figure 1) [23]. In the stabilization of metal–organic compounds, the dipolar interactions between carbonyl groups (CO \cdots CO) are also equally important in the stability of the crystal structures [24].

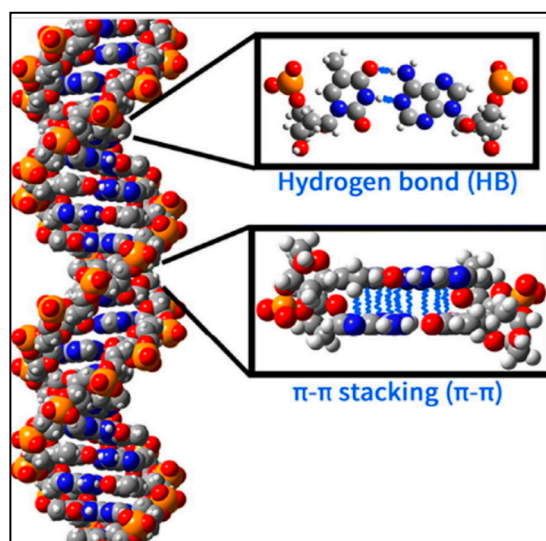


Figure 1. DNA double-helical structure stabilized by HB interactions and π -stacking.

The saturated aliphatic dicarboxylate moieties, as important flexible bridging ligands, can adopt conformational and coordination versatilities owing to their single-bonded carbon chains, which can be considered for the development of interesting metal–organic compounds [25,26]. The dicarboxylate anions can exhibit multiple coordination motifs such as uni-bidentate, bis-monodentate, bis-bidentate, tridentate, and tetradentate etc., thereby interconnecting metal centers to form polynuclear complexes [27,28]. Saturated dicarboxylic acids also serve as suitable H-bonding acceptors [29,30], resulting in the development of bridging metal–organic compounds with various desired self-assembled architectures [31,32]. As a consequence, adipic acid has evolved as a potential bridging ligand to form interesting coordination polymers with potential applications [33–35]. The dicarboxylate groups of fumarate anion (an unsaturated dicarboxylate) also have the ability to coordinate with the metal centers in multidentate fashion [36]. As a result, metal fumarate complexes have been explored with interesting structural topologies [37]. In recent times, a few boric acid-mediated metal–organic compounds have also been reported with desired applications [15,38].

In order to visualize the role of supramolecular interactions in polymeric complexes, we report herein the synthesis and crystal structures of two Na(I) polymers, namely, $\{Na(BA)_2(\mu-H_2O)_2\}_n\{adp\}_n$ (**1**) and $\{[Na_2(\mu-BA)(\mu-fum)(\mu-H_2O)_4](BA)\}_n$ (**2**) (where, BA = boric acid, adp = adipic acid, fum = fumarate), along with their characterization using FT-IR spectroscopy, TGA, and elemental analysis. The presence of various noncovalent interactions such as C-H \cdots H-C and parallel CO \cdots CO interactions stabilizes the 2D architecture of compound **1**. Fascinating dual enclathration of guest BA molecules within the supramolecular host cavities formed by O-H \cdots O hydrogen-bonding and noncovalent C-

H···H-C interactions provides rigidity to the crystal structure of compound **2**. To explore the energetic features and the characteristics of H-bonding interactions, we use QTAIM and NCI plot computational tools. The strength of the H-bonding interactions is investigated using the potential energy density in QTAIM, revealing the importance of $R_2^2(8)$ synthons in the crystal structures.

2. Experimental

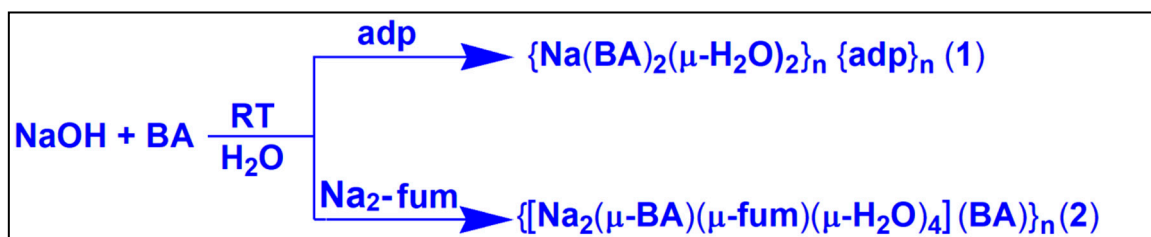
2.1. Materials and Methods

The chemicals used in the present study, namely, sodium hydroxide, boric acid, adipic acid, and fumaric acid, were purchased from commercial sources and used as received. We prepared the disodium salt of fumaric acid using standard laboratory methods. A Perkin Elmer 2400 Series II CHNS/O analyzer was used to carry out the elemental analysis of the compounds. KBr phase FT-IR spectra were recorded using a Bruker Alpha Infrared spectrophotometer (resolution = 4 cm^{-1} ; number of scans = 16), in the wavenumber range $4000\text{--}500\text{ cm}^{-1}$. Thermogravimetric studies were carried out under the flow of N_2 gas using a Mettler Toledo TGA/DSC1 STAR^c system at a heating rate of $10\text{ }^\circ\text{C}\cdot\text{min}^{-1}$. The TGA curves were recorded in the temperature range $25\text{--}1000\text{ }^\circ\text{C}$ with $2\text{ }\mu\text{g}$ resolution.

2.2. Syntheses

2.2.1. Synthesis of $\{\text{Na}(\text{BA})_2(\mu\text{-H}_2\text{O})_2\}_n\{\text{adp}\}_n$ (**1**)

Compound **1** was synthesized via the reaction of sodium hydroxide (0.040 g, 1.0 mmol) and boric acid (0.124 g, 2.0 mmol) in 10 mL of deionized water. The reaction mixture was mechanically stirred at room temperature for about 2 h. Then, adipic acid (1 mmol, 0.146 g) was slowly added, and the resulting solution was mechanically stirred for another hour (Scheme 1). The resulting solution was kept unperturbed in cooling conditions ($2\text{--}4\text{ }^\circ\text{C}$) for crystallization, from which block-shaped colorless single crystals were obtained after a few days. Yield: 0.282 g (86.02%). Analysis calculated for $\text{C}_6\text{H}_{19}\text{B}_2\text{NaO}_{12}$: C, 21.98%; H, 5.84%; found: C, 21.82%; H, 5.75%. IR (KBr pellet, cm^{-1}): 3401 (br), 3228 (sh), 3055 (s), 2963 (m), 2876 (m), 2860 (sh), 2579 (m), 1984 (m), 1922 (sh), 1697 (s), 1601 (s), 1506 (s), 1410 (s), 1288 (m), 1225 (s), 1163 (w), 1090 (m), 998 (w), 944 (m), 850 (s), 780 (w), 717 (s), 646 (sh), 537 (m) (s, strong; m, medium; w, weak; br, broad; sh, shoulder).



Scheme 1. Synthesis of compounds **1** and **2**.

2.2.2. Synthesis of $\{[\text{Na}_2(\mu\text{-BA})(\mu\text{-fum})(\mu\text{-H}_2\text{O})_4](\text{BA})\}_n$ (**2**)

For the synthesis of compound **2**, a mixture of sodium hydroxide (0.08 g, 2.0 mmol) and boric acid (0.124 g, 2.0 mmol) was mechanically stirred at room temperature for about 2 h in 10 mL of deionized water. Then, $\text{Na}_2\text{-fum}$ (0.160 g, 1.0 mmol) was added slowly, and the resulting solution was mechanically stirred for another hour (Scheme 1). The resulting solution was kept unperturbed in cooling conditions below $4\text{ }^\circ\text{C}$, from which block-shaped colorless single crystals were obtained after a few days. Yield: 0.295 g (82.86%). Analysis calculated for $\text{C}_4\text{H}_{16}\text{B}_2\text{Na}_2\text{O}_{14}$: C, 13.49%; H, 4.50%; found: C, 13.41%; H, 4.39%. IR (KBr pellet, cm^{-1}): 3447 (br), 3283 (sh), 2494 (s), 2140 (m), 2070 (w), 1690 (s), 1600 (s), 1427 (s), 1374 (s), 1265 (s), 1187 (s), 975 (s), 842 (m), 812 (m), 795 (m), 764 (m), 685 (s), 592 (sh) (s, strong; m, medium; w, weak; br, broad; sh, shoulder).

2.3. Crystallographic Data Collection and Refinement

Single-crystal XRD data of the compounds were recorded using a Bruker D8 Venture diffractometer with a Photon III 14 detector, using an Incoatec high-brilliance $\text{I}\mu\text{S}$ DIAMOND Cu tube. The Bruker APEX4 program was used for the data reduction and cell refinements [39]. Scaling and merging of the datasets of the wavelength were carried out using SADABS [39]. Crystal structures of the compounds were solved using the direct method and refined using the full-matrix least-squares technique with SHELXL-2018/3 [40] in WinGX [41] software. The non-hydrogen atoms of the crystal structures were refined with anisotropic thermal parameters using full-matrix least-squares calculations on F^2 . Hydrogen atoms were inserted at calculated positions and refined as riders. Diamond 3.2 software was used to draw the compounds [42]. Crystallographic data of the compounds are presented in Table 1.

Table 1. Crystallographic data and structure refinement details for compounds **1** and **2**.

Crystal Parameters	1	2
Empirical formula	$\text{C}_6\text{H}_{19}\text{B}_2\text{NaO}_{12}$	$\text{C}_4\text{H}_{16}\text{B}_2\text{Na}_2\text{O}_{14}$
Formula weight	327.82	355.77
Temperature (K)	100.0	294.0
Wavelength (\AA)	1.54178	1.54178
Crystal system	Triclinic	Orthorhombic
Space group	$P\bar{1}$	$Pnma$
a (\AA)	3.7723 (4)	14.0708 (12)
b (\AA)	8.6376 (9)	6.7995 (6)
c (\AA)	10.9248 (12)	14.9868 (12)
α ($^\circ$)	87.123 (4)	90
β ($^\circ$)	84.622 (4)	90
γ ($^\circ$)	82.919 (4)	90
Volume (\AA^3)	351.43 (7)	1433.9 (2)
Z	1	4
Calculated density (g/cm^3)	1.549	1.648
Absorption coefficient (mm^{-1})	1.543	1.950
$F(000)$	172.0	736.0
Crystal size (mm^3)	$0.26 \times 0.24 \times 0.15$	$0.39 \times 0.26 \times 0.21$
θ range for data collection ($^\circ$)	8.134 to 137.124	8.62 to 136.55
Index ranges	$-4 \leq h \leq 4$, $-10 \leq k \leq 10$, $-13 \leq l \leq 13$	$-16 \leq h \leq 16$, $-8 \leq k \leq 7$, $-18 \leq l \leq 18$
Reflections collected	7484	15,582
Unique data (R_{int})	1276	1421
Refinement method	Full-matrix least squares on F^2	Full-matrix least-squares on F^2
Data/restraints/parameters	1276/0/118	1421/0/161
Goodness-of-fit on F^2	1.074	1.065
Final Rindices [$I > 2\sigma(I)$] $R1/wR2$	0.0422/0.1152	0.0228/0.0616
Rindices (all data) $R1/wR2$	0.0427/0.1161	0.0229/0.0617
Largest diff. peak and hole ($\text{e}\cdot\text{\AA}^{-3}$)	0.31 and -0.24	0.25 and -0.19

CCDC 2213579 and 2213580 contain the supplementary crystallographic data for the compounds **1** and **2** respectively. These data can be obtained free of charge at <http://www.ccdc.cam.ac.uk> or from the Cambridge Crystallographic Data Center (12 Union Road, Cambridge CB2 1EZ, UK; Fax: (+44) 1223-336-033; or E-mail: deposit@ccdc.cam.ac.uk).

2.4. Theoretical Methods

The single-point calculations were carried out using the Turbomole 7.7 program [43] and the PBE0-D3/def2-TZVP [44–46] level of theory. The crystallographic coordinates were used to evaluate the interactions in compounds **1** and **2** since we were interested in studying the H-bonding interactions in the solid state. Since the structures were polymeric, finite

models extracted from the solid-state structures were selected to study the formation of the H-bonding interactions. The Bader's "Atoms in molecules" theory (QTAIM) [47] and noncovalent interaction plot (NCI Plot) [48] were used to study the interactions discussed herein using the Multiwfn program [49] and represented using the VMD visualization software [50]. For the calculation of the H-bond energies, we used the equation proposed by Espinosa et al. ($E = \frac{1}{2}Vr$) [51].

3. Results

3.1. Synthesis and General Aspects

$\{\text{Na}(\text{BA})_2(\mu\text{-H}_2\text{O})_2\}_n\{\text{adp}\}_n$ (**1**) was synthesized via a reaction involving NaOH, BA, and adp in 1:2:1 ratio at room temperature in deionized water. Similarly, $\{[\text{Na}_2(\mu\text{-BA})(\mu\text{-fum})(\mu\text{-H}_2\text{O})_4](\text{BA})\}_n$ (**2**) was prepared by reacting NaOH, BA, and Na₂-fum in 2:2:1 ratio at room temperature in deionized water. Compounds **1** and **2** were soluble in water, as well as common organic solvents. The crystal structure of compound **2** was already reported by Ozer et al. [52] (Table S1). However, we synthesized the compound by employing a comparatively simple synthetic pathway at room temperature. We also explored the detailed structural characteristics of the compound, which revealed the unusual dual enclathration of BA moieties in the supramolecular host cavity of the compound (*vide infra*). Moreover, the energetic features of the H-bonding interactions were investigated in the crystal structure using computational tools (*vide infra*).

3.2. Crystal Structure Analysis

The molecular structure of compound **1** is depicted in Figure 2. Table S2 contains the bond lengths and bond angles around the Na(I) centers. The compound crystallized in the triclinic $P\bar{1}$ space group. Compound **1** comprises two 1D polymeric chains. The first one possesses Na(I) centers bridged by two water molecules. Two BA molecules are also coordinated with the Na(I) centers. Thus, each Na(I) center is hexacoordinated with two O atoms from the BA molecules (O2B and O2B') and four O atoms from the bridged water molecules (O1W, O1W', O1W'', and O1W'''). The coordination geometry around each Na(I) center is ideal octahedron, where the axial positions are filled by two bridged water molecules, whereas the equatorial sites are occupied by the other bridged water molecules and the two O atoms of BA moieties. Moreover, the second 1D polymeric chain holds adp molecules bridged by the hydrogen atom of adp (H3A). X-ray crystallographic analysis indicates that the 1D polymeric chain of Na(I) centers possesses a crystallographic inversion center at the midpoint of two neighboring Na(I) centers. The 1D polymeric chain of adp also possesses crystallographic inversion at the midpoint of the C–C bond of adp.

The 1D polymeric chain of compound **1** consisting of the Na(I) centers is stabilized by noncovalent intramolecular O–H...O hydrogen-bonding interactions (Figure S1 see Supplementary materials). The O4B atoms of the coordinated boric acid molecules are involved in O–H...O hydrogen-bonding interactions with the bridged water molecule O1W, with O1W–H1WB...O4B having a distance of 2.09 Å.

The 1D polymeric chains of the compound **1** also propagate along the ab plane to stabilize the layered assembly aided by CH...HC and parallel CO...CO interactions (Figure S2). H atoms (H4AA, H4AB, H5AA, and H5AB) of the adp molecules are involved in CH...HC bonding interactions, with H4AA...H4AB and H5AA...H5AB separations of 2.40 and 2.34 Å respectively. There are unusual parallel CO...CO interactions among the carbonyl groups of adp molecules having a Cg1 (defined by centroid of C2A and O1A)...Cg2 (defined by centroid of C2A and O1A) separation of 3.77 Å.

The 1D polymeric chains of Na(I) centers of the compound propagate along the crystallographic ab plane and form the layered assembly stabilized by O–H...O hydrogen-bonding interactions (Figure 3). O–H...O interactions are observed between O2B and O3B atoms of coordinated boric acid molecules (O2B–H2B...O3B = 1.95 Å).

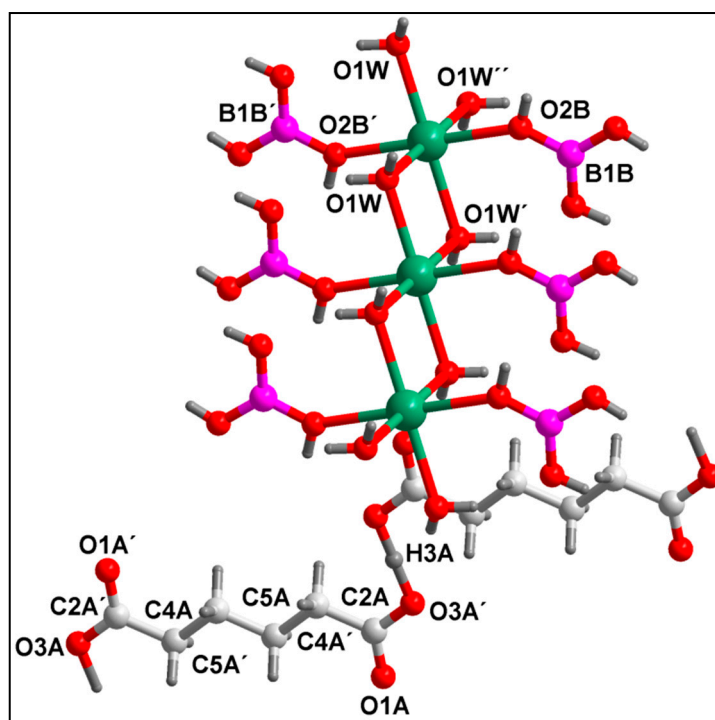


Figure 2. Molecular structure of the polymeric complex 1.

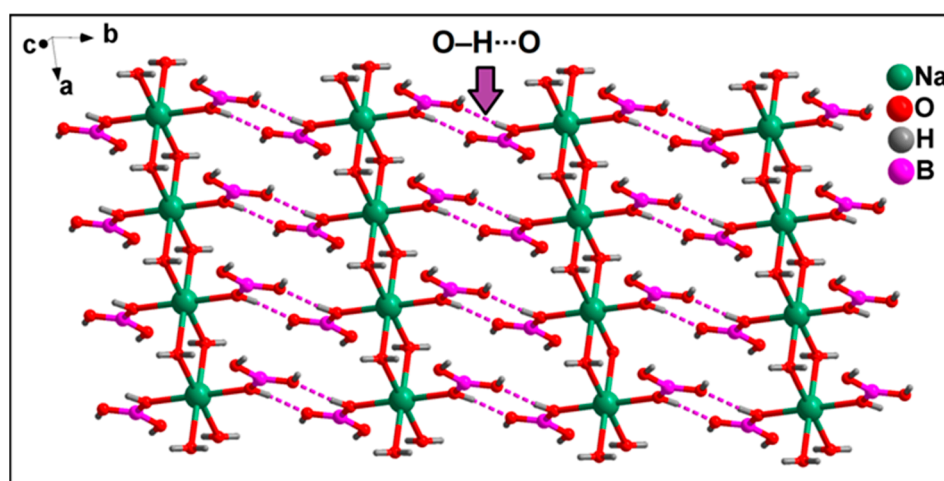


Figure 3. Layered assembly of compound 1 involving the polymeric chains of Na(I) centers assisted by O-H...O hydrogen-bonding interactions along the crystallographic ab plane.

Both the polymeric chains of adp moieties and Na(I) centers are interconnected along the bc plane to stabilize the layered assembly (Figure 4b) aided by C-H...O and O-H...O interactions. The -CH (C4AH4A) moiety of adp is involved in C-H...O hydrogen-bonding interactions with O4B atom of coordinated BA of the Na(I) centers, having a C4A-H4A...O4B distance of 2.74 Å. The supramolecular ring motif formed is represented using Etter's graph set notation, i.e., $R_2^2(8)$ [53].

Moreover, the O1A and O3A atoms of adp moieties are involved in O-H...O hydrogen-bonding interactions with coordinated BA moieties of the Na(I) centers, having O3B-H3B...O1A and O4B-H4B...O3A distances of 1.89 and 2.06 Å, respectively (Figure 4a). These interactions were further studied theoretically (vide infra).

Figure 5 depicts the molecular structure of compound 2. Tables S3 and S4 contains bond lengths and bond angles around Na(I) centers. Compound 2 crystallized in the or-

thorhombic $Pnma$ space group. The crystal structure of compound **2** consists of a 1D polymeric chain and one uncoordinated BA moiety (Figure 5). The polymeric chain possesses two crystallographically unique Na(I) centers (Na1 and Na2) having a similar coordination environment with minor differences in bond lengths and bond angles. Two neighboring Na(I) centers are bridged by two water molecules, along with one BA and one fum moiety. Na1 centers are hexacoordinated with four bridged water molecules (O1W, O1W', O2W, and O2W'), the O1 atom from the bridged fum, and the O2A atom from the bridged BA molecule.

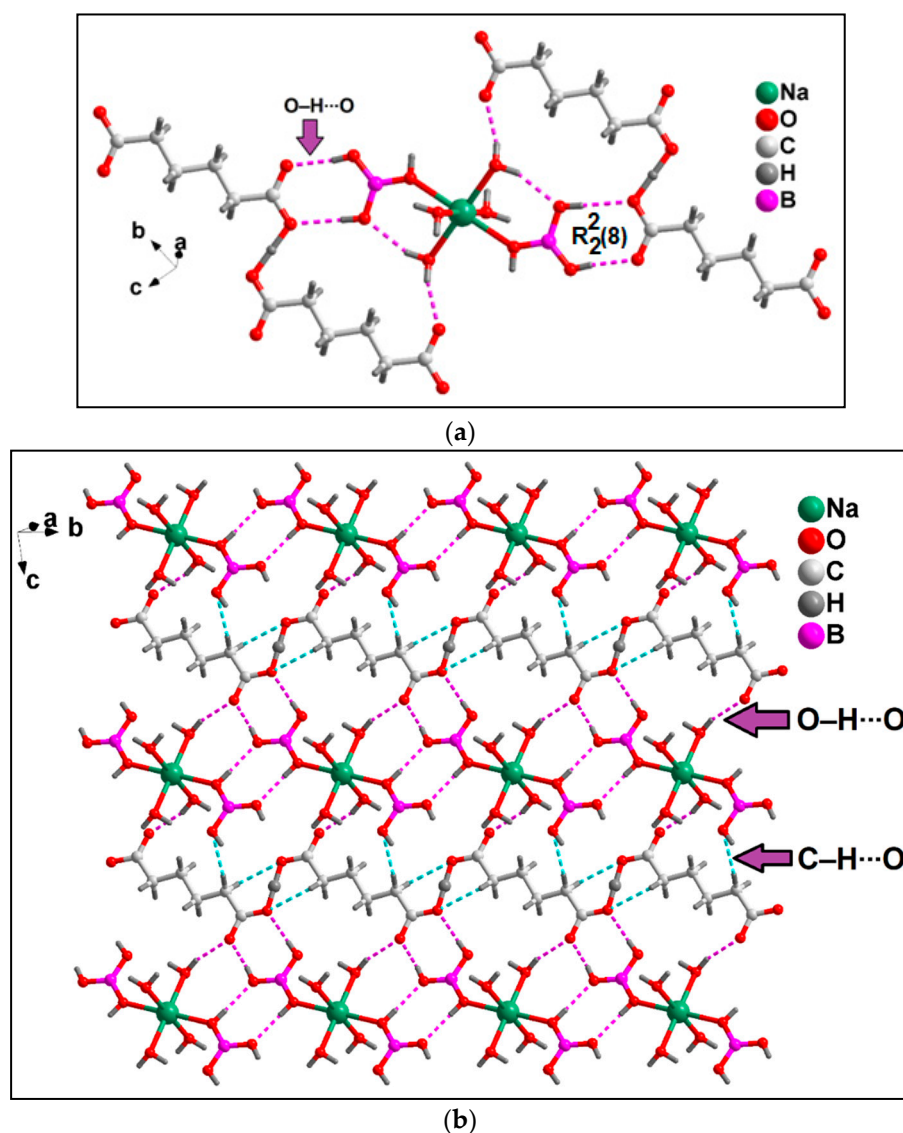


Figure 4. (a) Partial view of the layered assembly of compound **1** stabilized by O-H...O hydrogen-bonding interactions. (b) Layered assembly of compound **1** involving both the polymeric chains of adp and Na(I) centers along the crystallographic bc plane.

However, Na2 centers are also hexacoordinated with four bridged water molecules (O1W, O1W', O2W, and O2W'), the O8 atom from bridged fum, and the O3A atom from the bridged BA molecule. The coordination geometry around each Na1 center is distorted octahedron, where the axial sites are filled up by O1 and O2A, while equatorial sites are filled by the four bridged water molecules. The O1W, O1W', O2W, and O2W' atoms deviate from the mean equatorial plane with a rms deviation of 0.0304 Å. Similarly, for Na2 centers, axial sites are filled by O8 and O3A, whereas the equatorial positions are filled by four bridged water molecules. The structural properties such as bond lengths and bond

angles of the compound are found to be slightly different from those of the previously reported compound (Tables S3 and S4).

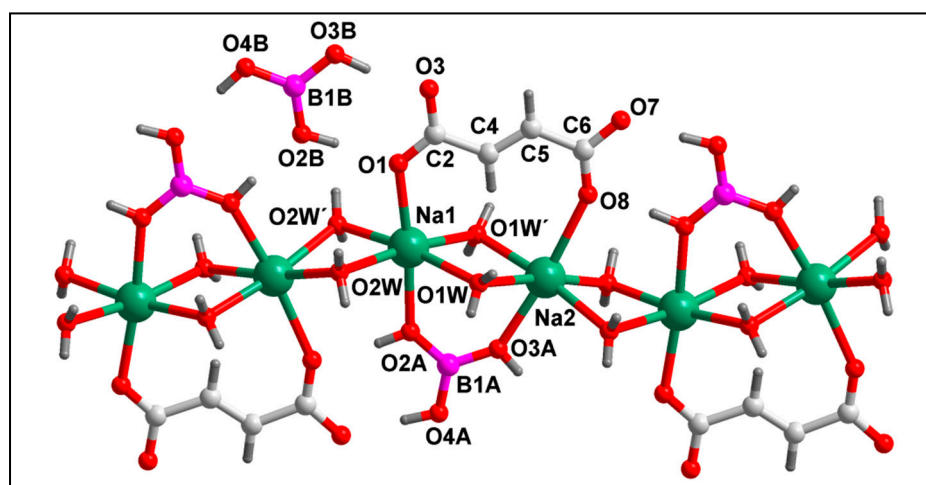


Figure 5. Molecular structure of polymeric complex 2.

Analysis of the crystal packing of compound 2 revealed that O7 and O8 atoms of bridged fum are involved in intramolecular O-H...O interactions with bridged BA moieties, having O4A-H4A...O7 and O2A-H2A...O8 distances of 1.71 and 1.80 Å, respectively (Figure 6). The uncoordinated BA moiety is involved in intermolecular O-H...O interactions with the O1 and O3 atoms of bridged fum, having O3B-H3B...O3 and O2B-H2B...O1 distances of 1.75 and 1.77 Å, respectively. Moreover, uncoordinated and bridged BA moieties are also involved in O-H...O interactions (O3A-H3A...O2B = 1.86 Å, O4B-H4B...O4A = 1.81 Å) (Figure 6). The H-bonded ring motif formed in compound 2 is represented by Etter's graph set notation, i.e., $R_2^2(8)$ [53]. These $R_2^2(8)$ synthons were further studied theoretically (vide infra).

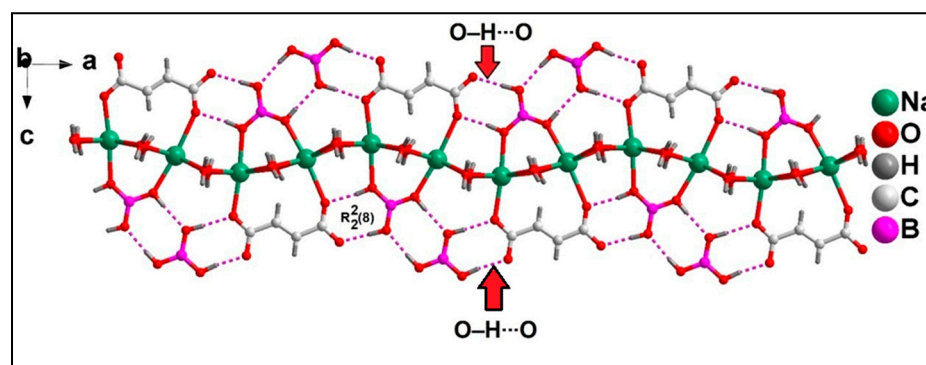


Figure 6. The 1D polymeric chain of compound 2 involving intramolecular and intermolecular O-H...O hydrogen-bonding interactions.

Unusual dual enclathration of lattice boric acid moieties within the supramolecular host cavity aided by O-H...O and C-H...C interactions (Figure 7a) stabilize the layered assembly of the compound. The O7 atom of bridging fum and the O2W molecule are involved in O-H...O interactions (O2W-H2WB...O7 = 2.08 Å). Noncovalent C-H...C contacts are observed between -C5H5 moieties and C4 atoms of fum of two neighboring 1D polymeric chains, having a C5-H5...C4 distance of 3.88 Å [C(sp²)-C(sp²), C5...C4 = 3.95 Å]. Moreover, enclathration of two BA moieties takes place with the help of O-H...O interactions involving the O1 and O3 atoms of bridging fum, as well as the O3A and O4A atoms of bridging BA (O2B-H2B...O1 = 1.77 Å, O3B-H3B...O3 = 1.75 Å, O3A-H3A...O2B = 1.87 Å,

and $O4B-H4B\cdots O4A = 1.82 \text{ \AA}$). In addition, $O3B$ and $O4B$ atoms of enclathrated boric acids are also involved in $O-H\cdots O$ interactions with bridging $O1W$ and $O2W$ molecules, having $O2W-H2WA\cdots O3B$ and $O1W-H1WB\cdots O4B$ distances of 1.92 and 2.22 \AA , respectively (Table 2).

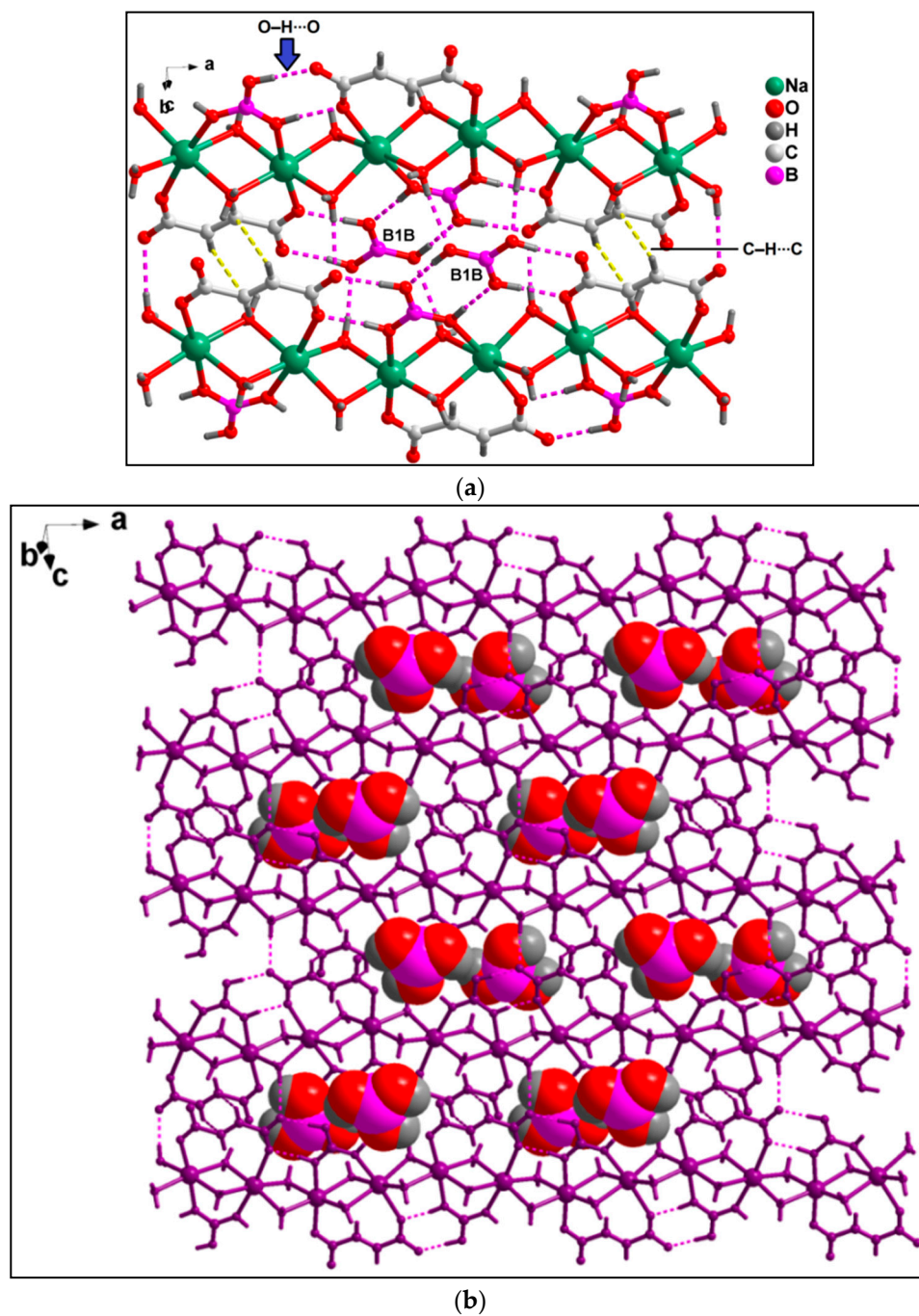


Figure 7. (a) Dual enclathration of lattice BA molecules in the supramolecular host cavity formed of **2**. (b) The 2D architecture of **2** along the crystallographic ac plane aided by dual enclathration of lattice BA molecules within the supramolecular host cavity.

Table 2. Selected hydrogen bond distances (Å) and angles (°) for compounds **1** and **2**.

D–H···A	d(D–H)	d(D···A)	d(H···A)	<(DHA)
Compound 1				
O1W–H1WB···O4B ^{#1}	0.86	2.91	2.09	159.4
O2B–H2B···O3B ^{#3}	0.82	2.769	1.95	175
C4A–H4AB···O3A	0.99	3.02	2.64	103.1
C4A–H4AA···O4B	0.99	3.726	2.74	175.1
O3B–H3B···O1A ^{#2}	0.77	2.658	1.89	175
O4B–H4B···O3A ^{#2}	0.83	2.891	2.06	176.5
Compound 2				
O4A–H4A···O7 ^{#6}	0.89	2.6	1.71	178
O2A–H2A···O8 ^{#6}	0.87	2.665	1.8	174
O2W–H2WB···O7 ^{#4}	0.83	2.902	2.08	168.9
O2B–H2B···O1	0.88	2.646	1.77	178
O3B–H3B···O3	0.9	2.638	1.75	172
O3A–H3A···O2B ^{#7}	0.81	2.677	1.87	177
O4B–H4B···O4A ^{#6}	0.87	2.682	1.82	176
O2W–H2WA···O3B ^{#5}	0.86	2.777	1.92	175.3
O1W–H1WB···O4B ^{#5}	0.8	3.016	2.22	169.1

^{#1} 1 + X, +Y, +Z; ^{#2} −1 + X, 1 + Y, +Z; ^{#3} 1 − X, 1 − Y, 1 − Z; ^{#4} 1 − X, −1/2 + Y, 1 − Z; ^{#5} 1/2 − X, 1 − Y, −1/2 + Z; ^{#6} −1/2 + X, 3/2 − Y, 1/2 − Z; ^{#7} 1/2 + X, 3/2 − Y, 1/2 − Z.

Interestingly, dual enclathration of uncoordinated BA molecules within the supramolecular host cavities forms the 2D architecture of **2** along the ac plane (Figure 7b). Such dual enclathration of BA moieties within supramolecular host cavities is rare.

3.3. FT-IR Spectroscopy

The FT-IR spectra of compounds **1** and **2** (KBr phase) were recorded in the region 4000–500 cm^{−1} (Figure 8). The comparatively broad absorption peaks in both compounds at around 3401 and 3447 cm^{−1} can be attributed to O–H stretching vibrations of water molecules [54,55]. FT-IR spectra exhibited peaks due to ρ_r (H₂O) (712 cm^{−1}) and ρ_w (H₂O) (645 cm^{−1}), which indicates the presence of coordinated water molecules [55]. For **1**, strong absorption bands at 1601 and 1410 cm^{−1} are due to the asymmetric and symmetric stretching vibrations of the carboxylate moieties of adp [56]. Peaks at 2963 and 2876 cm^{−1} in **1** are due to the asymmetric and symmetric C–H stretching vibrations of –CH₂ moieties of adp [57,58]. Peaks for C–C stretching of the adp can be observed at 1225 (asymmetric) and 1090 (symmetric) cm^{−1} in **1** [59]. $\Delta\nu = \nu_{\text{asym}} - \nu_{\text{sym}}$ of fum (greater than 200 cm^{−1}) can be attributed to the monodentate coordination of the carboxylate groups to the Na(I) centers in compound **2** [60]. The medium-intensity peaks at 812 and 795 cm^{−1} in compound **2** are due to the OCO bending vibrations of fum [60]. The sharp peak at 1710 cm^{−1} in **1** indicates that the carboxylate group of adp does not undergo deprotonation, whereas its absence in **2** supports the deprotonation of carboxylate moieties [61].

3.4. Thermogravimetric Analysis

TG analysis of the compounds was carried out in the temperature range 25–1000 °C under N₂ atmosphere at a heating rate of 10 °C/min (Figure 9). For compound **1**, in the temperature range 50–100 °C, two coordinated water molecules were decomposed (observed = 11.56%; calculate = 10.98%) [62]. In the temperature range 101–270 °C, one coordinated BA molecule was decomposed with the observed weight loss of 17.04% (calculated = 18.86%) [63]. The observed weight loss of 62.24% (calculated = 62.76%) in the temperature range 271–930 °C can be attributed to the loss of one coordinate BA molecule and one coordinated adp moiety [63,64]. For compound **2**, four coordinated water molecules were decomposed between 51 and 180 °C (observed = 19.80%, calculated = 20.24%) [62]. In

the temperature range 181–326 °C, two BA moieties and one fum moieties were lost (observed = 66.20%, calculated = 67.36%) [63,65].

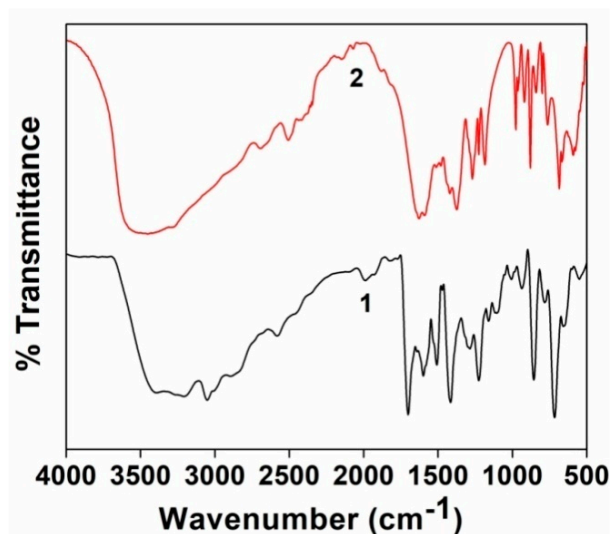


Figure 8. FT-IR spectra of compounds 1 and 2.

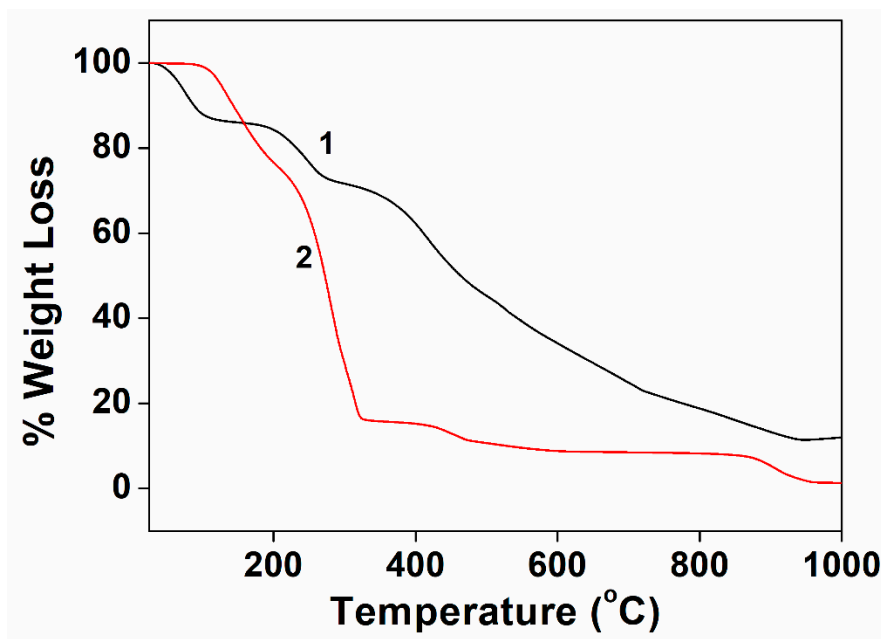


Figure 9. Thermogravimetric curves of the compounds 1 and 2.

3.5. Theoretical Study

The theoretical study was devoted to the analysis of the H-bonding interactions observed involving boric acid, both as a donor and as an acceptor, that are relevant to the stability of the solid state of the compounds. The polymeric nature of the complexes complicated the theoretical analysis. Therefore, we used finite models of the compounds and took advantage of the QTAIM method that allows the quantification of the H-bonds using the potential energy density values at the bond critical points (CPs). To do so, the V_r values at the bond critical points that characterize each synthon and the equation $E = \frac{1}{2}V_r$ were used. As a representative fragment of compound 1, we used the model represented in Figure 10a, composed of a central Na atom coordinated to four water molecules and two monodentate boric acids and two sets of H-bridged adipate dimers. Such a model included the most relevant H-bonds observed in compound 1. The QTAIM analysis combined with

the NCI plot analysis is shown in Figure 10a, where each H-bond is characterized by a bond critical point (CP, red sphere) and a bond path connecting the H-atoms to the O-atoms. Moreover, green (weak) and blue (strong) RDG isosurfaces also characterize the H-bonds. One important synthon corresponds to the supramolecular $R_2^2(8)$ ring, where the BA forms two strong H-bonds with one fum. The formation energy of this synthon is -11.7 kcal/mol due to the contribution of both $\text{OH}\cdots\text{OH}$ -bonds, where the boric acid acts as a double H-bond donor. The equatorial water molecules participate in two H-bonds, one intramolecular with the BA and the other one intermolecular with the adp. The intermolecular one is stronger (-4.6 kcal/mol), likely due to the anionic nature of the H-bond acceptor.

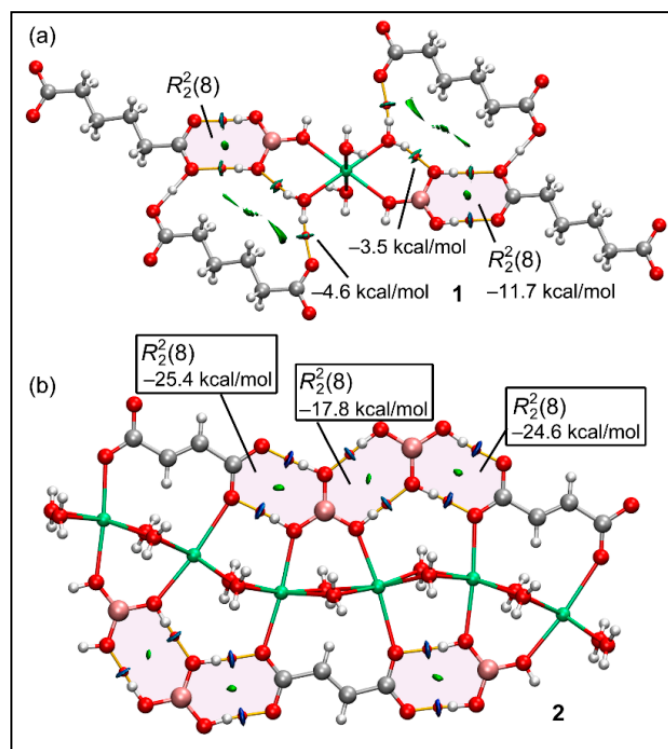


Figure 10. QTAIM (bond CPs in red and bond paths as orange lines) and NCI plot analysis (RDG = 0.6, $\rho_{\text{cut-off}} = 0.04$, color range -0.04 a.u. $\leq (\text{sign}\lambda_2)\rho \leq 0.04$ a.u.).

The oligomeric model used for compound 2 is shown in Figure 10b, composed of a total of six hexacoordinated sodium atoms, three coordinated BAs, two free BAs, and three bidentate fum ligands. It is interesting to highlight the formation of three different $R_2^2(8)$ synthons in the solid state, which have very large interaction energies. One of the synthons is generated by the interaction of the coordinated and non-coordinated BAs, with a formation energy of -17.8 kcal/mol. The other two $R_2^2(8)$ synthons correspond to the interaction of the non-coordinated and coordinated BAs with the fumarate ligands. Both synthons exhibit very strong formation energies due to the anionic nature of the H-bond donor and the strong acidity of the H-bond donor atoms. In fact, the strongest synthon (-25.4 kcal/mol) corresponds to the coordinated BA, where the acidity of these OH groups is enhanced by the coordination to the sodium cation.

4. Conclusions

Two Na(I) polymeric compounds were synthesized and characterized using single-crystal X-ray diffraction, FT-IR, and TG analyses. Compound 1 comprises two polymeric chains: one water-bridged polymeric Na(I) chain and another chain formed by adp molecules with bridging hydrogen atoms. Compound 2 contains a polymeric Na(I) chain bridged by BA and fum moieties. The coordination environment around the Na(I) atoms in

both polymers is octahedral. Unconventional supramolecular contacts, namely, C-H...H-C and parallel CO...CO interactions, stabilize the layered assembly of compound **1**. Interesting dual enclathration of BA molecules within the supramolecular hosts formed by O-H...O and C-H...H-C interactions stabilizes the crystal structure of compound **2**. The structure-directing H-bonded noncovalent interactions in the crystal structures were further studied theoretically using the combined QTAIM/NCI plot method, and the energies were estimated using the V_r energy predictor. It is demonstrated that the formation of a strong structure directing H-bonded $R_2^2(8)$ synthons in the compounds is relevant for the layered assemblies of the compounds.

Supplementary Materials: The following supporting information can be downloaded at <https://www.mdpi.com/article/10.3390/cryst13060895/s1>: Table S1: Comparison of crystal parameters of compound **2** with the already reported compound; Table S2: Selected bond lengths (Å) and bond angles (°) of Na(I) centers in compound **1**; Tables S3 and S4: Selected bond lengths (Å) and bond angles (°), respectively, of Na(I) centers in compound **2** and the previously reported compound (CCDC 1455138); Figure S1: The 1D polymeric chain of compound **1** stabilized by intramolecular O-H...O hydrogen bonding interactions; Figure S2: Layered assembly of compound **1** involving polymeric chain of *adp* moieties assisted by unusual CH...HC and parallel CO...CO interactions along the crystallographic *ab* plane.

Author Contributions: Conceptualization, A.F. and M.K.B.; methodology, A.F. and M.K.B.; software, A.F. and R.M.G.; formal analysis, A.F.; investigation, T.B., K.K.D. and R.M.G.; data curation, M.B.-O.; writing—original draft preparation, T.B., K.K.D. and M.K.B.; writing—review and editing, M.K.B.; visualization, A.F.; supervision, M.K.B.; project administration, A.F. and M.K.B.; funding acquisition, A.F. and M.K.B. All authors have read and agreed to the published version of the manuscript.

Funding: Financial support from ASTEC, DST, the Government of Assam (grant number ASTEC/S&T/192(177)/2020-2021/43), and the Government of Spain, MICIU/AEI (projects No. EQC2018-00426 5-P and PID2020-115637GB-I00) is gratefully acknowledged. The authors thank IIT-Guwahati for TG data.

Data Availability Statement: Not applicable.

Conflicts of Interest: The authors declare no conflict of interest. The funders had no role in the design of the study; in the collection, analyses, or interpretation of data; in the writing of the manuscript; or in the decision to publish the results.

References

1. Engel, E.R.; Scott, J.L. Advances in the Green Chemistry of Coordination Polymer Materials. *Green Chem.* **2020**, *22*, 3693–3715. [[CrossRef](#)]
2. Biradha, K.; Ramanan, A.; Vittal, J.J. Coordination Polymers versus Metal–Organic Frameworks. *Cryst. Growth Des.* **2009**, *9*, 2969–2970. [[CrossRef](#)]
3. Ghosh, A.K.; Hazra, A.; Mondal, A.; Banerjee, P. Weak Interactions: The Architect behind the Structural Diversity of Coordination Polymer. *Inorg. Chim. Acta* **2019**, *488*, 86–119. [[CrossRef](#)]
4. Bureekaew, S.; Shimomura, S.; Kitagawa, S. Chemistry and Application of Flexible Porous Coordination Polymers. *Sci. Technol. Adv. Mater.* **2008**, *9*, 14108. [[CrossRef](#)] [[PubMed](#)]
5. Scaeteanu, G.V.; Maxim, C.; Badea, M.; Olar, R. Zinc(II) Carboxylate Coordination Polymers with Versatile Applications. *Molecules* **2023**, *28*, 1132. [[CrossRef](#)]
6. Ou, Y.C.; Zhong, R.M.; Wu, J.Z. Recent Advances in Structures and Applications of Coordination Polymers Based on Cyclohexanepolycarboxylate Ligands. *Dalton Trans.* **2022**, *51*, 2992–3003. [[CrossRef](#)] [[PubMed](#)]
7. Ding, B.; Solomon, M.B.; Leong, C.F.; D’Alessandro, D.M. Redox-Active Ligands: Recent Advances towards Their Incorporation into Coordination Polymers and Metal–Organic Frameworks. *Coord. Chem. Rev.* **2021**, *439*, 213891. [[CrossRef](#)]
8. Fromm, K.M. Coordination Polymer Networks with S-Block Metal Ions. *Coord. Chem. Rev.* **2008**, *252*, 856–885. [[CrossRef](#)]
9. Das, B.C.; Chokkalingam, P.; Masilamani, P.; Shukla, S.; Das, S. Stimuli-Responsive Boron-Based Materials in Drug Delivery. *Int. J. Mol. Sci.* **2023**, *24*, 2757. [[CrossRef](#)]
10. Córdova-Chávez, R.I.; Carrasco-Ruiz, M.F.; Rodríguez-Vera, D.; Pérez-Capistran, T.; Tamay-Cach, F.; Scorei, I.R.; Abad-García, A.; Soriano-Ursúa, M.A. Boron-Containing Compounds for Prevention, Diagnosis, and Treatment of Human Metabolic Disorders. *Biol. Trace Elem. Res.* **2023**, *201*, 2222–2239.

11. Ji, L.; Zhou, H. Recent developments in the synthesis of bioactive boron-containing compounds. *Tetrahedron Lett.* **2021**, *82*, 153411–153426. [[CrossRef](#)]
12. Ali, F.; Hosmane, N.S.; Zhu, Y. Boron Chemistry for Medical Applications. *Molecules* **2020**, *25*, 828. [[CrossRef](#)] [[PubMed](#)]
13. Lopalco, A.; Lopodota, A.A.; Laquintana, V.; Denora, N.; Stella, V.J. Boric Acid, a Lewis Acid with Unique and Unusual Properties: Formulation Implications. *J. Pharm. Sci.* **2020**, *109*, 2375–2386. [[CrossRef](#)] [[PubMed](#)]
14. Tan, W.; Chen, T.; Liu, W.; Ye, F.; Zhao, S. Design and fabrication of boric acid functionalized hierarchical porous metal-organic frameworks for specific removal of cis-diol-containing compounds from aqueous solution. *Appl. Surface Sci.* **2021**, *535*, 147714. [[CrossRef](#)]
15. Cebula, J.; Fink, K.; Boratyński, J.; Goszczyński, T.M. Supramolecular chemistry of anionic boron clusters and its applications in biology. *Coord. Chem. Rev.* **2023**, *477*, 214940. [[CrossRef](#)]
16. Alkorta, I.; Elguero, J.; Frontera, A. Not only hydrogen bonds: Other noncovalent interactions. *Crystals* **2020**, *10*, 180. [[CrossRef](#)]
17. Bhattacharyya, M.K.; Saha, U.; Dutta, D.; Frontera, A.; Verma, A.K.; Sharma, P.; Das, A. Unconventional DNA-Relevant π -Stacked Hydrogen Bonded Arrays Involving Supramolecular Guest Benzoate Dimers and Cooperative Anion- π/π - π/π -Anion Contacts in Coordination Compounds of Co(II) and Zn(II) Phenanthroline: Experimental and Theoretical Studies. *New J. Chem.* **2020**, *44*, 4504–4518. [[CrossRef](#)]
18. Desiraju, G.R. Chemistry beyond the Molecule. *Nature* **2001**, *412*, 397–400. [[CrossRef](#)]
19. Crabtree, R.H. Hypervalency, Secondary Bonding and Hydrogen Bonding: Siblings under the Skin. *Chem. Soc. Rev.* **2017**, *46*, 1720–1729. [[CrossRef](#)]
20. Karas, L.J.; Wu, C.-H.; Das, R.; Wu, J.I.-C. Hydrogen Bond Design Principles. *WIREs Comput. Mol. Sci.* **2020**, *10*, e1477. [[CrossRef](#)]
21. Mahmudov, K.T.; Kopylovich, M.N.; da Silva, M.F.C.G.; Pombeiro, A.J.L. Non-Covalent Interactions in the Synthesis of Coordination Compounds: Recent Advances. *Coord. Chem. Rev.* **2017**, *345*, 54–72. [[CrossRef](#)]
22. Desiraju, G.R.; Steiner, T. *The Weak Hydrogen Bond: In Structural Chemistry and Biology*; Oxford University Press: Oxford, UK, 2001.
23. Gutiérrez-Flores, J.; Ramos, E.; Mendoza, C.I.; Hernández-Lemus, E. Electronic Properties of DNA: Description of Weak Interactions in TATA-Box-like Chains. *Biophys. Chem.* **2018**, *233*, 26–35. [[CrossRef](#)]
24. Allen, F.H.; Baalham, C.A.; Lommerse, J.P.M.; Raithby, P.R. Carbonyl–Carbonyl Interactions Can Be Competitive with Hydrogen Bonds. *Acta Crystallogr.* **1998**, *54*, 320–329. [[CrossRef](#)]
25. Contejean, Z.I.; LaDuca, R.L. Nitroaromatic-Detecting Zinc and Cadmium Coordination Polymers with Methyl-Substituted Aliphatic Dicarboxylate and 4,4'-Dipyridylamine Ligands and Diverse Topologies. *J. Solid State Chem.* **2018**, *266*, 44–53. [[CrossRef](#)]
26. White, C.L.; LaDuca, R.L. Nickel Adipate Coordination Polymers with Isomeric Dipyridylamide Ligands: Topological Disorder and Divergent Magnetic Properties. *CrystEngComm.* **2016**, *18*, 6789–6797. [[CrossRef](#)]
27. Ignatyev, I.; Kondratenko, Y.; Fundamensky, V.; Kochina, T. Synthesis and Characterization of Cobalt(II) Complexes with Triethanolamine and Succinate and/or Nitrate Anions. *Transit. Met. Chem.* **2018**, *43*, 127–136. [[CrossRef](#)]
28. Forlin, E.; Lanza, A.; Nicola, C.D.; Monari, M.; Gazzano, M.; Nestola, F.; Pettinari, C.; Pandolfo, L. 1D and 3D Coordination Polymers Based on the Cu₃(M₃-OH)(μ -Pz)₃ and Cu(Hpz)₃ SBUs Connected by the Flexible Glutarate Dianion. *Inorg. Chim. Acta* **2018**, *470*, 385–392. [[CrossRef](#)]
29. Biswas, C.; Jana, A.D.; Drew, M.G.B.; Mostafa, G.; Ghosh, A. Segregated Self-Assembly and Pillaring Action of Aliphatic Dicarboxylic Acids in the Super Structure of Cu–Picolinate Complexes. *Polyhedron* **2009**, *28*, 653–660. [[CrossRef](#)]
30. Kathalikkattil, A.C.; Damodaran, S.; Bisht, K.K.; Suresh, E. Hydrogen Bonded Binary Molecular Adducts Derived from Exobidentate N-Donor Ligand with Dicarboxylic Acids: Acid \cdots imidazole Hydrogen-Bonding Interactions in Neutral and Ionic Heterosynths. *J. Mol. Struct.* **2011**, *985*, 361–370. [[CrossRef](#)]
31. Dutta, B.; Maity, S.; Ghosh, S.; Sinha, C.; Mir, M.H. An Acetylenedicarboxylato-Bridged Mn(II)-Based 1D Coordination Polymer: Electrochemical CO₂ Reduction and Magnetic Properties. *New J. Chem.* **2019**, *43*, 5167–5172. [[CrossRef](#)]
32. Arici, M.; Erer, H.; Karaçam, S.; Yeşilel, O.Z.J. Coordination polymers based on 3,3-dimethylglutarate and 1,4-bis((1H-imidazol-1-yl) methyl) benzene: Hydrothermal synthesis and characterizations. *J. Solid State Chem.* **2019**, *277*, 811–818. [[CrossRef](#)]
33. Chandra, A.; Dutta, B.; Pal, K.; Jana, K.; Sinha, C. Designing of an Adipic Acid Bridged Zn(II) Coordination Polymer: Synthesis and Biological Study. *J. Mol. Struct.* **2021**, *1243*, 130923. [[CrossRef](#)]
34. Zhang, J.W.; Xu, S.; Liu, S.N.; Hu, J.; Qiao, Y.X.; Liu, B.Q. Two Series of Substituent-Group-Directed Adipate-Based Lanthanide Coordination Polymers: Syntheses, Structures, Photoluminescence, and Magnetism. *Eur. J. Inorg. Chem.* **2020**, *2020*, 1233–1241. [[CrossRef](#)]
35. Song, Y.; Yan, Y.; Zhang, H.; Wang, X. Synthesis and Structural Characterization of a Novel 2D Supramolecular Lead Coordination Polymer with Phenanthroline Derivate and Adipic Acid. *Main Group Met. Chem.* **2021**, *44*, 239–242. [[CrossRef](#)]
36. Zhang, G.; Yang, G.; Ma, J.S. Hydrothermal Syntheses and Characterization of Novel 3D Open-Framework and 2D Grid Lanthanide Fumarates: Ln₂(Fum)₃(H₂fum)(H₂O)₂ (Ln = Ce or Nd), [Sm₂(Fum)₃(H₂O)₄](H₂O)₃, and [Yb₂(Fum)₃(H₂O)₄](H₂O)₂. *Cryst. Growth Des.* **2006**, *6*, 933–939. [[CrossRef](#)]
37. Gogoi, A.; Das, A.; Frontera, A.; Verma, A.K.; Bhattacharyya, M.K. Energetically Significant Unconventional π - π Contacts Involving Fumarate in a Novel Coordination Polymer of Zn(II): In-Vitro Anticancer Evaluation and Theoretical Studies. *Inorg. Chim. Acta* **2019**, *493*, 1–13. [[CrossRef](#)]

38. Ozer, D.; Köse, D.A.; Şahin, O.; Oztas, N.A. Synthesis and Characterization of Boric Acid Mediated Metal-Organic Frameworks Based on Trimesic Acid and Terephthalic Acid. *J. Mol. Struct.* **2017**, *1141*, 261–267. [[CrossRef](#)]
39. APEX3, SAINT, SADABS and XP; Bruker AXS Inc.: Madison, WI, USA, 2015.
40. Sheldrick, G.M. Crystal Structure Refinement with SHELXL. *Acta Crystallogr. Sect. A Found. Crystallogr.* **2008**, *64*, 112–122. [[CrossRef](#)]
41. Farrugia, L.J. WinGX and ORTEP for Windows: An update. *J. Appl. Crystallogr.* **1999**, *32*, 837–838. [[CrossRef](#)]
42. Brandenburg, K. *Diamond 3.1f*; Crystal Impact GbR: Bonn, Germany, 2008.
43. Ahlrichs, R.; Bär, M.; Häser, M.; Horn, H.; Kölmel, C. Electronic Structure Calculations on Workstation Computers: The Program System Turbomole. *Chem. Phys. Lett.* **1989**, *162*, 165–169. [[CrossRef](#)]
44. Adamo, C.; Barone, V. Toward Reliable Density Functional Methods without Adjustable Parameters: The PBE0 Model. *J. Chem. Phys.* **1999**, *110*, 6158–6170. [[CrossRef](#)]
45. Grimme, S.; Antony, J.; Ehrlich, S.; Krieg, H. A Consistent and Accurate ab initio Parametrization of Density Functional Dispersion Correction (DFT-D) for the 94 Elements H–Pu. *J. Chem. Phys.* **2010**, *132*, 154104–154119. [[CrossRef](#)] [[PubMed](#)]
46. Weigend, F. Accurate Coulomb-Fitting Basis Sets for H to Rn. *Phys. Chem. Chem. Phys.* **2006**, *8*, 1057–1065. [[CrossRef](#)] [[PubMed](#)]
47. Bader, R.F.W. Atoms in Molecules. *Chem. Rev.* **1991**, *91*, 893–928. [[CrossRef](#)]
48. Johnson, E.R.; Keinan, S.; Mori-Sánchez, P.; Contreras-García, J.; Cohen, A.J.; Yang, W. Revealing Noncovalent Interactions. *J. Am. Chem. Soc.* **2010**, *132*, 6498–6506. [[CrossRef](#)] [[PubMed](#)]
49. Lu, T.; Chen, F. Multiwfn: A Multifunctional Wavefunction Analyzer. *J. Comput. Chem.* **2012**, *33*, 580–592. [[CrossRef](#)]
50. Humphrey, J.W.; Dalke, A.; Schulten, K. VMD: Visual molecular dynamics. *J. Mol. Graph.* **1996**, *14*, 33–38. [[CrossRef](#)]
51. Espinosa, E.; Molins, E.; Lecomte, C. Hydrogen Bond Strengths Revealed by Topological Analyses of Experimentally Observed Electron Densities. *Chem. Phys. Lett.* **1998**, *285*, 170–173. [[CrossRef](#)]
52. Ozer, D.; Köse, D.A.; Sahin, O.; Oztas, N.A. Study of Structural, Surface and Hydrogen Storage Properties of Boric Acid Mediated Metal (Sodium)-Organic Frameworks. *J. Mol. Struct.* **2018**, *1157*, 159–164. [[CrossRef](#)]
53. Etter, M.C. Encoding and decoding hydrogen-bond patterns of organic compounds. *Acc. Chem. Res.* **1990**, *23*, 120–126. [[CrossRef](#)]
54. Nashre-ul-Islam, S.M.; Dutta, D.; Guha, A.K.; Bhattacharyya, M.K. An Unusual Werner Type Clathrate of Mn(II) Benzoate Involving Energetically Significant Weak CH \cdots C Contacts: A Combined Experimental and Theoretical Study. *J. Mol. Struct.* **2019**, *1175*, 130–138. [[CrossRef](#)]
55. Manna, S.C.; Mistri, S.; Jana, A.D. A Rare Supramolecular Assembly Involving Ion Pairs of Coordination Complexes with a Host–Guest Relationship: Synthesis, Crystal Structure, Photoluminescence and Thermal Study. *CrystEngComm* **2012**, *14*, 7415–7422. [[CrossRef](#)]
56. Nath, H.; Dutta, D.; Sharma, P.; Frontera, A.; Verma, A.K.; Barceló-Oliver, M.; Devi, M.; Bhattacharyya, M.K. Adipato Bridged Novel Hexanuclear Cu(II) and Polymeric Co(II) Coordination Compounds Involving Cooperative Supramolecular Assemblies and Encapsulated Guest Water Clusters in a Square Grid Host: Antiproliferative Evaluation and Theoretical Studies. *Dalton Trans.* **2020**, *49*, 9863–9881. [[CrossRef](#)] [[PubMed](#)]
57. Tan, X.-F.; Zhou, J.; Zou, H.-H.; Xiao, H.-P.; Tang, Q.; Jiang, T.; Zhang, X. Synthesis, Crystal Structures and Properties of a Series of Lanthanide Adipates [Ln₂(Ad)₃(H₂O)₄] (Ln = Y³⁺, Ho³⁺, Er³⁺, Tm³⁺). *J. Clust. Sci.* **2016**, *27*, 2025–2033. [[CrossRef](#)]
58. Jumanath, E.C.; Pradyumn, P.P. Thermal Degradation and Spectroscopic Studies of Single-Crystalline Organometallic Calcium Adipate Monohydrate. *J. Therm. Anal. Calorim.* **2020**, *140*, 567–575. [[CrossRef](#)]
59. Jumanath, E.C.; Pradyumn, P.P. Growth, Characterization and Dielectric Property Studies of Zinc Adipate Dihydrate Crystals. *AIP Conf. Proc.* **2019**, *2082*, 1–5.
60. Deacon, G.B.; Phillips, R.J. Relationships between the Carbon–Oxygen Stretching Frequencies of Carboxylate Complexes and the Type of Carboxylate Coordination. *Coord. Chem. Rev.* **1980**, *33*, 227–250. [[CrossRef](#)]
61. Nakamoto, K. *Infrared and Raman Spectra of Inorganic and Coordination Compounds, Part B: Applications in Coordination, Organometallic, and Bioinorganic Chemistry*; John Wiley & Sons: Hoboken, NJ, USA, 2009.
62. Bora, S.J.; Das, B.K. Synthesis, structure and properties of a fumarate bridged Ni (II) coordination polymer. *J. Mol. Struct.* **2011**, *999*, 83–88. [[CrossRef](#)]
63. Hernández, M.F.; Suárez, G.; Cipollone, M.; Conconi, M.S.; Aglietti, E.F.; Rendtorff, N.M. Formation, Microstructure and Properties of Aluminum Borate Ceramics Obtained from Alumina and Boric Acid. *Ceram. Int.* **2017**, *43*, 2188–2195. [[CrossRef](#)]
64. Wang, C.G.; Xing, Y.H.; Li, Z.P.; Li, J.; Zeng, X.Q.; Ge, M.F.; Niu, S.Y. A Series of Three-Dimensional Lanthanide-Rigid-Flexible Frameworks: Synthesis, Structure, and Luminescent Properties of Coordination Polymers with 2,5-Pyridine Dicarboxylic Acid and Adipic Acid. *Cryst. Growth Des.* **2009**, *9*, 1525–1530. [[CrossRef](#)]
65. Téllez-López, A.; Sánchez-Mendieta, V.; Jaramillo-García, J.; Rosales-Vázquez, L.D.; García-Orozco, I.; Morales-Luckie, R.A.; Escudero, R.; Morales-Leal, F. Modification of the Structure and Magnetic Properties of Fumarato-Bridged Mn Coordination Polymers through Different Dimethyl-2,2'-Bipyridine Co-Ligands. *Transit. Met. Chem.* **2016**, *41*, 879–887. [[CrossRef](#)]

Disclaimer/Publisher's Note: The statements, opinions and data contained in all publications are solely those of the individual author(s) and contributor(s) and not of MDPI and/or the editor(s). MDPI and/or the editor(s) disclaim responsibility for any injury to people or property resulting from any ideas, methods, instructions or products referred to in the content.